Image Fusion Method based on Non-Subsampled Contourlet Transform

Hui Liu
School of Science, Jiangxi University of Science and Technology, 341000 Ganzhou, China
Email: lxyliuhui@163.com

***Abstract*—Considering human visual system and characteristics of images, a novel image fusion strategy is presented for panchromatic high resolution image and multispectral image in non-subsampled contourlet transform (NSCT) domain. The NSCT can give an asymptotic optimal representation of edges and contours in image by virtue of its characteristics of good multiresolution, shiftinvariance, and high directionality. An intensity component addition strategy based on NMF algorithm is introduced into NSCT domain to preserve spatial resolution and color content. Experiments show that the proposed algorithm can not only reduce computational complexities, but achieve better performances than other mentioned techniques both in visual point and statistics compared with the traditional principle component analysis (PCA) method, intensity-hue-saturation (IHS) transform technique, wavelet transform weighted fusion method, corresponding wavelet transform-based fusion method, and contourlet transform-based fusion method.**

***Index Terms*—Image fusion, Non-Subsampled Contourlet Transform, Non-Negative Matrix Factorization.**

I. INTRODUCTION

Image fusion is a process by combining two or more source images from different modalities or instruments into a single image with more information. The successful fusion is of great importance in many applications, such as remote sensing, computer vision, medical imaging, and so on. In the pixel level fusion, some generic requirements can be imposed on the fusion results [1]:

1) The fused image should preserve all relevant information contained in the source images as closely as possible.

2) The fused process should not introduce any artifacts or inconsistencies, which can distract or mislead the human observer, or any subsequent image processing steps.

3) In the fused image, irrelevant features and noise should be suppressed to a maximum extent.

Panchromatic (PAN) images of high spatial resolution can provide detailed geometric information, such as shapes, features, and structures of objects of the earth's surface. While multispectral (MS) images with usually lower resolution are used to obtain spectral information necessary for environmental applications. The different objects within images of high spectral resolution are easily identified. Data fusion methods aim to obtain the images with high spatial and spectral resolution, simultaneously. The PAN and MS remote sensing image fusion is different from other fusion applications, such as image fusion in military missions or computer-aided quality control. The specificity is to preserve the spectral information for subsequent classification of ground cover. The classical fusion methods are principle component analysis (PCA), intensity-hue-saturation (IHS) transform, etc. In recent years, with the development of wavelet transform theory and multi-resolution analysis, two-dimensional separable wavelets have been widely used in image fusion and have achieved good results[2−4].

Thus, the fusion algorithms mentioned above can hardly make it by themselves. They usually cause some characteristic degradation, spectral loss, or color distortion. For example, the IHS transform can enhance texture information and spatial features of fused images, but suffers from much spectral distortion. The PCA method will lose some original spectral features in the process of principal component substitution. The wavelet transform (WT) can preserve spectral information efficiently but cannot express spatial characteristics well. Furthermore, the isotropic wavelets are scant of shift-invariance and multi-directionality and fail to provide an optimal expression of highly anisotropic edges and contours in images.

Image decomposition is an important link of image fusion and affects the information extraction quality, even the whole fusion quality. In recent years, along with the development and application of the wavelet theory, the favorable time-frequency localization to express local signal makes wavelet a candidate in multi-sensor image fusion. However, wavelet bases are isotropy and of limited directions and fail to represent high anisotropic edges and contours in images well. The MGA emerges, which comes from wavelet multi-resolution, but beyond it. The MGA can take full advantage of the geometric regularity of image intrinsic structures and obtain the asymptotic optimal representation. As an MGA tool, the contourlet transform (CT) has the characteristics of localization, multi-direction, and anisotropy[5]. The CT can give the asymptotic optimal representation of

Manuscript received February 20, 2011; revised March 22, 2011; accepted June 25, 2011.

doi:10.4304/jsw.7.12.2816-2822

contours and has been applied in image fusion effectively. However, the CT is lack of shift-invariance and results in artifacts along the edges to some extends.

Until recently, the multi-resolution decomposition based algorithms have been widely used in multi-source image fusion field, and effectively overcame the problem of spectrum distortion. In which, wavelet transformation enjoys great time-frequency analytical features and is the focus of multi-source image fusion. In 2002, Do and Vetteri proposed a flexible contourlet transform method that may efficiently detect the geometric structure of images attribute to its properties of multi-resolution, local and directionality [1]. But spectrum aliasing phenomenon occurs posed by unfavorable smoothness of basis function. Cunha et al. put forward a NSCT (Non-Subsampled Contourlet Transform) method [2] in 2006, improvements has been made in solving limitations of contourlet, and it was the transformation with attributes of shift-invariant, multi-scale and multi-directionality [3].

NMF (Non-Negative Matrix Factorization) was a new matrix analysis method [4], presented by Lee and Seung in 1999, and has been proved converged to its local minimum in 2000 [5]. The non-negative constraints imposed on NMF lead to extensive applications, and it has been successfully applied to image analysis, text clustering, data mining, speech processing, robot control, face recognition, biomedical and chemical engineering. In current references, Miao et al. applied NMF in multi-focus image fusion [6]; Novak et al. utilized NMF in language modeling for grammar identification [7]; Feng et al. used NMF in face recognition program [8, 9]. Owing to the pixels are generally non-negative in digital image processing, hence, the results arising from NMF directly express specific physical meaning.

An improved NMF algorithm is proposed, and applied in image fusion program combine with NSCT, in which the novel NMF approach is performed to fuse the low-frequency information in NSCT domain while the fusion of high-frequency details can be realized by adopting the technique called as NHM (Neighborhood Homogeneous Measurement). The experimental results demonstrate that the fusion method proposed can effectively extract useful information of source images and inject it into the final fused one which owns better visual effect and occupies less CPU time comparing with algorithm in [10].

This paper discusses the fusion of multispectral and panchromatic remote sensing images. An improved NMF algorithm is proposed and applied The rest of this paper is organized as follows. Section 1 gives the NSCT of images. Section 2 introduces NMF fusion algorithm and it's transform. Section 3 proposes a new algorithm based on the combination ANMF and NSCT. Section 4 reports about the fusion experiments tested on PAN and MS image sets using the proposed algorithm. Conclusions are drawn in Section 5.

II. NON-SUBSAMPLED CONTOURLET TRANSFORM

A. Contourlet Transform

Do and Vetterli proposed a "true" two-dimensional transform called contourlet transform, which is based on nonseparable filter banks and provides an efficient directional multiresolution image representation. The CT expresses image by first applying a multiscale transform, followed by a local directional transform to gather the nearby basis functions at the same scale into linear structures. For example, the Laplacian pyramid (LP) is first used to capture the point discontinuities, and then followed by a direction filter banks (DFB) to link point discontinuities into linear structures. In particular, contourlets have elongate supports at various scales, directions, and aspect ratios. The contourlets satisfy anisotropy principle and can capture intrinsic geometric structure information of images and achieve better expression than discrete wavelet transform (DWT), especially for the edges and contours.

However, because of the downsampling and upsampling, the CT is lack of shift-invariance and results in ringing artifacts. But, the shift-invariance is desirable in image analysis applications, such as edge detection, contour characterization, image fusion, etc[7].

Especially, during the realization of the CT, the analysis filter banks and synthesis filter banks of LP decomposition are nonseparable bi-orthogonal filter banks with band width larger than $\pi/2$. Based on multisampled rate theory, downsample on filtered image may result in lowpass and highpass frequency aliasing. Therefore, the frequency aliasing affects lie in directional subbands, which comes from the highpass subbands filtered by DFB. The frequency aliasing will result in information in a direction to appear in different directional subbands at the same time. This must weaken the directional selectivity of contourlets.

B. Non-subsampled Contourlet Transform

NSCT is proposed on the grounds of contourlet conception [1], which discards the sampling step during image decomposition and reconstruction stages. Furthermore, NSCT achieves the ability of shift-invariant, multi-resolution and multi-dimension for image presentation by using non-sampled filter bank iteratively.

The structure of NSCT consists of two parts: NSP (Non-Subsampled Pyramid) and NSDFB (Non-Subsampled Directional Filter Banks). NSP, a multi-scale decomposed structure, is a dual-channel non-sampled filter that is developed from àtrous algorithm. And it does not contain subsampled process. (Fig. 1, a) shows the framework of NSP, for each decomposition of next level, the filter $H(z)$ is firstly sampled using upper-two sampling method, the sampling matrix is $D = (2, 0; 0, 2)$. Then, low-frequency components derive from last level are decomposed iteratively just as its predecessor did. As a result, a tree-like structure that enables multi-scale decomposition is achieved. NSDFB is constructed based on the fan-out DFB presented by Bamberger and Smith. It does not include both the super-sampling and sub-sampling steps, but rely on sampling the relative filters in DFB by treating $D = (1, 1; 1, -1)$, which is illustrated in (Fig. 1, b).

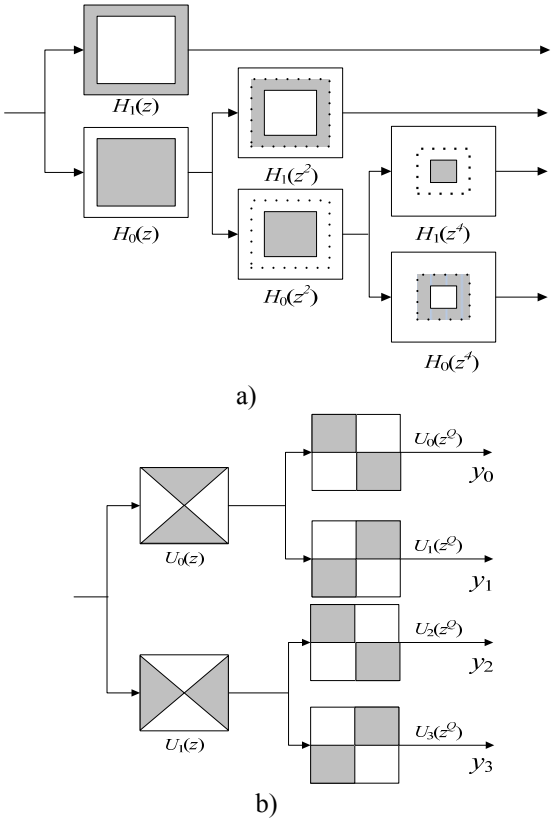

Fig.1. Diagram of NSP and NSDFB: a – three-levels NSP; b – decomposition of NSDFB

III IMPROVED NONNEGATIVE MATRIX FACTORIZATION

A. Nonnegative Matrix Factorization

NMF is a recently developed matrix analysis algorithm [4, 5], which can not only describes low-dimensional intrinsic structure in high-dimensional space, but achieves linear representation for original sample data by imposing non-negativity constraints. It makes all the components non-negative (i.e., pure additive description) after being decomposed as well as realizes the non-linear dimension reduction, simultaneously. NMF is defined as:

Conduct N times of investigation on a M-dimensional stochastic vector v first, then record these data as v_j, j = 1,2,…, N, let $V = [\, V_{\bullet 1}, V_{\bullet 2}, V_{\bullet N}\,]$, where $V_{\bullet j} = v_j, j = 1,2,\ldots, N$. NMF is required to find a non-negative $M \times L$ base matrix $W = [W_{\bullet 1}, W_{\bullet 2},\ldots, W_{\bullet N}]$ and a $L \times N$ coefficient factor $H = [H_{\bullet 1}, H_{\bullet 2},\ldots, H_{\bullet N}\,]$, so that $V \approx WH$ [4]. The equation can also be wrote in a more intuitive form of $V_{\cdot j} \approx \sum_{i=1}^{L} W_{\cdot i} H_{\cdot j}$ where L should be chose to satisfy $(M + N)$ $L < MN$.

In the purpose of finding the appropriate factors W and H in solving NMF problem, the commonly used two objective functions are depicted as [5]:

$$E(V \,\|\, WH) = \| V - WH \|_F^2 = \sum_{i=1}^{M}\sum_{j=1}^{N} (V_{ij} - (WH)_{ij})^2 \,, \quad (1)$$

$$D(V \,\|\, WH) = \sum_{i=1}^{M}\sum_{j=1}^{N} (V_{ij} \log \frac{V_{ij}}{(WH)_{ij}} - V_{ij} + (WH)_{ij}) \,, \quad (2)$$

In respect to formulas (1) and (2), $\forall i$, a, j subject to $W_{ia} > 0$ and $H_{aj} > 0$. $\|\bullet\|_F$ is the Frobenius norm, (1) is called as the Euclid distance while (2) is referred to as K-L divergence function. Note that, Find the approximate solution to $V \approx WH$ is considered equal to the optimization of above mentioned two objective functions.

B. Accelerated Nonnegative Matrix Factorization

Roughly speaking, NMF algorithm has high time complexity that results in limited advantage for overall performance of algorithm, so that the introduction of improved iteration rules used to optimize the NMF is extremely crucial to promote the efficiency. In the point of algorithm optimization, NMF is the majorization problem that contents non-negative constraint. Until now, a wide range of decomposition algorithms have been investigated on the basis of non-negative constraint, such as the multiplicative iteration rules, interactive non-negative least squares, gradient method and projected gradient [11]. In which the projected gradient approach is capable of reducing the time complexity of iteration to realize the NMF applications in mass data condition. In addition, these works are distinguished by meaningful physical significance, effective sparse data, enhanced classification accuracy and striking time decreasing. We propose a modified version of projected gradient NMF that will greatly reduce the complexity of iterations, the main idea of the algorithm is listed blow:

As we known, the Lee-Seung algorithm continuously updates H and W, which fixing the other, by taking a step in a certain weighted negative gradient direction, namely:

$$H_{ij} \leftarrow H_{ij} - \eta_{ij} \left[\frac{\partial f}{\partial H}\right]_{ij} \equiv H_{ij} + \eta_{ij} (W^T A - W^T WH)_{ij} \,, \quad (3)$$

$$W_{ij} \leftarrow W_{ij} - \varsigma_{ij} \left[\frac{\partial f}{\partial W}\right]_{ij} \equiv W_{ij} + \varsigma_{ij} (AH^T - WHH^T)_{ij} \,, \quad (4)$$

where η_{ij} and ζ_{ij} are individual weights for the corresponding gradient elements, which are expressed like follows:

$$\eta_{ij} = \frac{H_{ij}}{(W^T WH)_{ij}} \,,\ \varsigma_{ij} = \frac{W_{ij}}{(WHH^T)_{ij}} \,, \quad (5)$$

and then the updating formulas:

$$H_{ij} \leftarrow H_{ij} \frac{(W^T A)_{ij}}{(W^T WH)_{ij}} \,,\ W_{ij} \leftarrow W_{ij} \frac{(AH^T)_{ij}}{(WHH^T)_{ij}} \,, \quad (6)$$

We notice that the optimal H related to a fixed W can be obtained, column by column, by independently:

$$\min \ \frac{1}{2} \| Ae_j - WHe_j \|_2^2 \quad \text{s.t.} \quad He_j \geq 0 \,, \quad (7)$$

where e_j is the j^{th} column of the $n\times n$ identity matrix. Similarly, we can also acquire the optimal W relative to a fixed H by solving, row by row:

$$\min \ \frac{1}{2}\| A^T e_i - HW^T e_i \|_2^2 \quad \text{s.t.} \quad W^T e_i \geq 0, \tag{8}$$

where e_i is the i^{th} column of the $m\times m$ identity matrix. Actually, both problems (7) and (8) can be changed into an ordinary form:

$$\min \ \frac{1}{2}\| Ax - b \|_2^2 \quad \text{s.t.} \quad x \geq 0, \tag{9}$$

where $A \geq 0$ and $b \geq 0$. As the variables and given data are all nonnegative, the problem is therefore named as TNNLS (Totally Nonnegative Least Squares) issue.

We propose to revise the algorithm claimed in article [4] by using the same update rule with step-length α in [10] to the successive updates in improving the objective functions about the two TNNLS problems mentioned in formulas (7) and (8). As a result, this brings about a modified form of the Lee-Seung algorithm that successively updates the matrix H column by column and W row by row, with individual step-length α and β for each column of H and each row of W respectively. So we try to write the update rule as:

$$H_{ij} \leftarrow H_{ij} + \alpha_j \eta_{ij} (W^T A - W^T WH)_{ij}, \tag{10}$$

$$W_{ij} \leftarrow W_{ij} + \beta_j \varsigma_{ij} (AH^T - WHH^T)_{ij}, \tag{11}$$

where η_{ij} and ζ_{ij} are set equal to some small positive number as described in [10], α_j (j=1,2,…,n) and β_i (i=1,2,…,m) are step-length parameters can be computed as follows. Let $x > 0, q = A^T(b - Ax)$ and $p = [x./(A^T Ax)] \circ q$

where the symbol "./" means component-wise division and " $\circ$ " denotes multiplication. Then we introduce variable $\tau \in (0,1)$,

$$\alpha = \min\left(\frac{p^T q}{p^T A^T Ap}, \tau \max\{\hat{\alpha} : x + \hat{\alpha} p \geq 0\}\right), \tag{12}$$

We can easily obtain the step-length formula of α_j or β_i if (A, b, x) is replaced by (W, Ae_j, He_j) or (H^T, $A^T e_i$, $W^T e_i$), respectively. It is necessary to point out that q is the negative gradient of the objective function in [10], and the search direction p is a diagonally scaled negative gradient direction. The step-length α or β is either the minimum of the objective function in the search direction or a τ-fraction of the step to the boundary of the nonnegative quadrant.

Learning from literature [10] that both quantities, $p^T q/p^T A^T Ap$ and $\max\{\hat{a} : x + \hat{a}p \geq 0\}$ are greater than 1 in the definition of the step α. Thereby, we make $\alpha_j \geq 1$ and $\beta_i \geq 1$ by treating τ sufficiently close to 1. In our experiment, we choose τ = 0.99 which practically guarantees that α and β are always greater than 1.

Obviously, when $\alpha \leftarrow 1$ or $\beta \leftarrow 1$, update formulas (10) and (11) reduce to updates (3) and (4). In the algorithm, the step-length parameters are allowed to be greater than 1. It is this indicates that for any given (W, H), we can get at least the same or greater decrease in the objective function than the algorithm [10]. Hence, we will call the proposed algorithm the ANMF (accelerated NMF). Besides, the experiments in later section will demonstrate that the (ANMF) algorithm is indeed superior to that algorithm by generating better test results, especially when the amount of iterations is not too big.

IV THE ANMF AND NSCT COMBINED ALGORITHM

A. The Selection of Fusion Rules

As we known, the approximation characteristics of an image belongs to the low-frequency part, while the high-frequency counterpart exhibits detailed features of edge and texture. In this paper, NSCT method is utilized to separate the high and low components of source image in frequency domain, and then the two parts are dealt with different fusion rules according to their features. As a result, the fused image can be more complementary, reliable, clear and better understood.

By and large, the low-pass sub-band coefficients approximate original image at low-resolution, it generally represents image contour, but such high-frequency details as edge, region contour are not contained. So we take ANMF algorithm to achieve the low-pass sub-band coefficients which including holistic features of the two source images. The band-pass directional sub-band coefficients embody the particular information, edges, lines, and boundaries of region, the main function of which is to obtain spatial details as much as possible. In our paper, a NHM based local self-adaptive fusion method is adopted in band-pass directional sub-band coefficients acquisition phase, by calculating the identical degree of the corresponding neighborhood to determine the selection for band-pass coefficients fusion rules.

B. The Course of Image Fusion

Given that the two source images are A and B, with the same size, both have been registered, F is fused image. The fusion process is shown in (Fig. 2) and the steps are given as follows.

(1) Adopt NSCT to implement the multi-scale and multi-direction decompositions for source images A and B and the sub-band coefficients $\{C_{i_0}^A(m,n), C_{i,l}^A(m,n)\}$, $\{C_{i_0}^B(m,n), C_{i,l}^B(m,n)\}$ can be obtained.

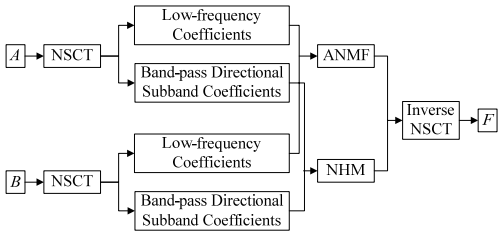

Fig. 2. Flowchart of fusion algorithm

(2) Construct matrix V on the basis of low-pass sub-band coefficients $C_{i_0}^A(m,n)$ and $C_{i_0}^B(m,n)$:

$$V=[v_A,v_B]=\begin{bmatrix} v_{1A} & v_{1B} \\ v_{2A} & v_{2B} \\ \cdots & \cdots \\ v_{nA} & v_{nB} \end{bmatrix}, \tag{13}$$

where v_A and v_B are column vectors consisting of pixels come from A and B respectively according to principles of row by row. n is the number of pixels of source image. And perform ANMF algorithm described above on V, from which W that is actually the low-pass sub-band coefficients of fused image F is separated. We set maximum iteration number as 1000 with $\tau = 0.99$.

The fusion rule NHM is applied to band-pass directional sub-band coefficients $C_{i,l}^A(m,n)$, $C_{i,l}^B(m,n)$ of source images A, B. The NHM is calculated as:

$$NHM_{i,j}(m,n)\frac{2\times\{\sum_{(k,j)\in N_{i,j}(m,n)}|C_{i,j}^A(m,n)\times C_{i,j}^B(m,n)|\}}{E_{i,j}^A(m,n)+E_{i,j}^B(m,n)}, \tag{14}$$

where $E_{i,l}(m, n)$ is regarded as the neighborhood energy under resolution of 2^l in direction i, $N_{i,l}(m, n)$ is the 3 × 3 neighborhood centers at point (m, n). In fact, NHM quantifies the identical degree of correspond neighborhoods for two images, the higher the identical degree is, the greater the NHM value should be. Because $0 \le NHM_{i,l}(m, n) \le 1$, we define a threshold T, generally have it $0.5 < T < 1$. The smaller the T is, the image is more smooth, and less trace be found, but high-frequency content is prone to small too, which has been proved by a wealth of experiments. Therefore, the threshold is given as $T = 0.75$ by taking various factors into consideration. The fusion rule of band-pass directional sub-band coefficients is expressed as:

when $NHM_{i,l}(m, n) < T$,

$$\begin{cases} C_{i,l}^F(m,n)=C_{i,l}^A(m,n) \text{ if } E_{i,l}^A(m,n)\ge E_{i,l}^B(m,n) \\ C_{i,l}^F(m,n)=C_{i,l}^B(m,n) \text{ if } E_{i,l}^A(m,n)< E_{i,l}^B(m,n) \end{cases}$$

when $NHM_{i,l}(m, n) \ge T$,

$$C_{i,l}^F(m,n)=NHM_{i,l}(m,n)\times\max(C_{i,l}^F(m,n),C_{i,l}^A(m,n))+(1-NHM_{i,l}(m,n))\times\min(C_{i,l}^F(m,n),C_{i,l}^B(m,n))$$

(3) Perform inverse NSCT transform to fusion coefficients of F obtained from step (2) and get the ultimate fusion image F.

V. Experiments and Analysis

A. Fusion Experiments

To verify the effectiveness of the proposed algorithm, two groups of images are used under platform MATLAB 7.1. All source images must be of registered and with 256 gray levels. By comparison with three typical algorithms below, NSCT-based method (M1), NMF-based method (classic NMF, M2), weighted NMF based method (M3), we can learn more about the one presented in our paper.

In this context, we select the information entropy (IE), root mean square cross entropy (RCE), average grades (AG) and Q index as our evaluation metrics. The larger the IE is the more information is contained. RCE indicates the deviation degree between source images and the fused one, and is in inverse proportion to fusion effect. AG is capable of expressing the definition of the fused image, the larger the AG is, and clearer is the corresponding image. The Q index, refer to article [12], which measures the amount of edge information "transferred" from source images. Here, larger Q value means better algorithm performance.

B. Multi-focus Image Fusion

A pair of "Balloon" images are chose to be source images, both size are 200 by 160. As can be seen from (Fig. 3, a), the left side of the image is in focus while the other side is out of focus. The opposite appearance emerges in (Fig. 3, b). Three variant approaches, M1-M3 plus our method are applied to test the performance, and (Fig. 3, c - f) show the simulated results.

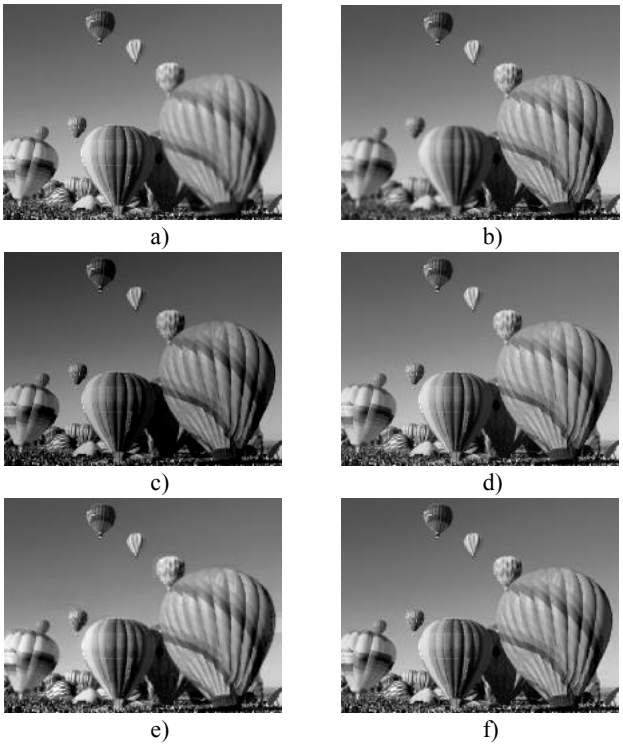

Fig. 3. Multi-focus source images and fusion results: a – left-focused image; b – right-focused image; c – fused image based on M1; d – fused image based on M2; e – fused image based on M3; f – fused image based on our method

From intuitive point of view, method M1 produces a poor intensity that makes (Fig. 3, c) is somewhat dim. On the contrary, the other three algorithms generate better performance on this aspect, but artifacts locate in the middle right of (Fig. 3, e) can be found. Compared with methods M2 and M3, although the definition of the bottom left region in our method is slightly lower than that of two algorithms, the holistic presentation is

superior to the two. Statistic results in Table 1 verified the visual effect.

Table 1 illustrates that the proposed method has advantage over others since three of four criteria, in details rendering and preserving respects, are superior to that of rest algorithms. The index IE of our method exceeds that of M1, M2 and M3 by 3.1%, 1.3% and 1.5% respectively. RCE index of the latter three methods are relatively high when against that of M1 in assessing deviation level. In index AG, the value of our method excels, which indicates that our method enjoys better visual effect. As for index Q, 0.9844 of our method means the most excellent performance when compared to value of former three algorithms.

TABLE 1.

COMPARISON OF THE FUSION METHODS FOR MULTI-FOCUS IMAGES

	M1	M2	M3	Proposed method
IE	7.3276	7.4594	7.4486	7.5608
RCE	0.2875	0.4940	0.4832	0.4539
AG	8.4581	8.2395	8.4595	8.6109
Q Index	0.9579	0.9723	0.9706	0.9844

C. Visible and Infrared Image Fusion

One set of registered visible and infrared images that a person is walking in front of a house are labeled as (Fig. 4, a) and (Fig. 4, b) with the size of 360 by 240. In which, (Fig. 4, a) has clear background but fails to detect foreground while (Fig. 4, b) highlights the person and house but its ability to render other surroundings is weak. Similar to the former experiment, four methods are utilized one by one to fuse these images.

We can find that the image based on method M1 is the worst in overall effect, especially a dark area around the person, which is partly caused by the significant differences between two source images. Method M2 produces more smooth details over M1, as a case in point, the road on the right side of the image and the grass on the other side can easily be recognized for the enhancement of intensity. Approximate effects displayed in (Fig. 4, e) and (Fig. 4, f) are achieved by using M3 and our method, from which we can easily distinguish most parts of the scene except the lighting beside the house in (Fig. 4, e) can hardly be observed. And it is difficult to judge the performance of M3 and our method through visual watching in case of the concrete data are not provided by Table 2.

In index IE, the value of our method is 6.7962 surpass that of M3 by 1.72% which indicate that our method has a distinct superiority over other algorithms as far as the information amount is concerned. As for RCE, the least deviation value is achieved by M1. In index AG, the optimal value is obtained on the basis of our method while that of M2 holds the final place. And the Q index of our method is still top of Table 2.

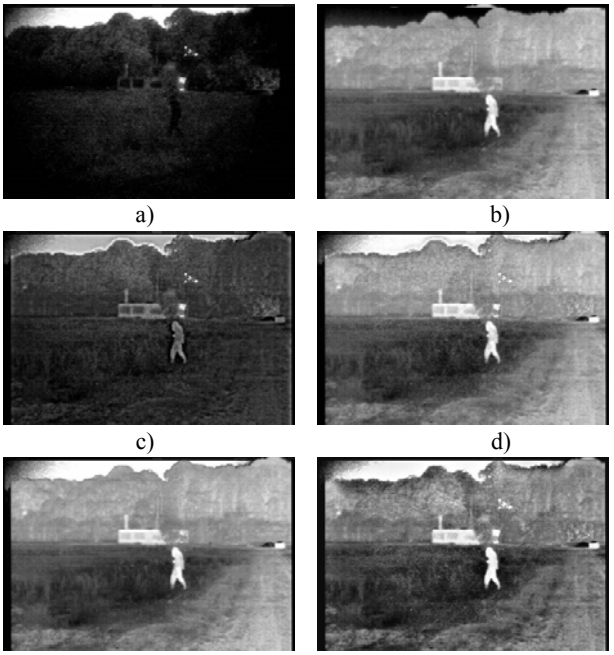

Fig. 4. Visible and infrared source images and fusion results: a – visible band image; b – Infrared band image; c – fused image based on M1; d – fused image based on M2; e – fused image based on M3; f – fused image based on our method

TABLE 2.

COMPARISON OF THE FUSION METHODS FOR VISIBLE AND INFRARED IMAGES

	M1	M2	M3	Proposed method
IE	6.2103	6.3278	6.7012	6.7962
RCE	1.3254	5.8970	4.4375	4.0261
AG	3.2746	3.0833	3.3695	3.5428
Q Index	0.9761	0.9784	0.9812	0.9903

D. Numerical Experiment on ANMF

In this section, we compare the performance of ANMF with that of algorithm presented in article [10] in order to prove its advantage, the algorithms are implemented in Matlab and applied to Equinox face database [13]. The contrast experiments are conducted 4 times, where p is as described above and n denotes for the number of images chosen from the face database. The Y axis of (Fig. 5) represents the number of iteration repeated by the two algorithms and the X axis is time consuming scale. We choose one group of these experiments and demonstrate the results in (Fig. 5) with p=100 and n=1000, in which algorithm in [10] is first performed for a given number of iterations and record the time elapsed and then run our algorithm until the time consumed is equivalent to that of former. We note that our algorithm offers improvement in all given time points, however, the relative improvement percentage of our method over algorithm in [10] goes down when increasing the number of iterations. Actually, the performance of our method increase about 36.8%, 26.4%, 15.7%, 12.6%, 7.5% respectively when comparing with it for five times. In other words, our method converges faster, especially at early stages, but the percentage tends to decline, which implies that this attribute is useful merely for real-time applications that without very large scale.

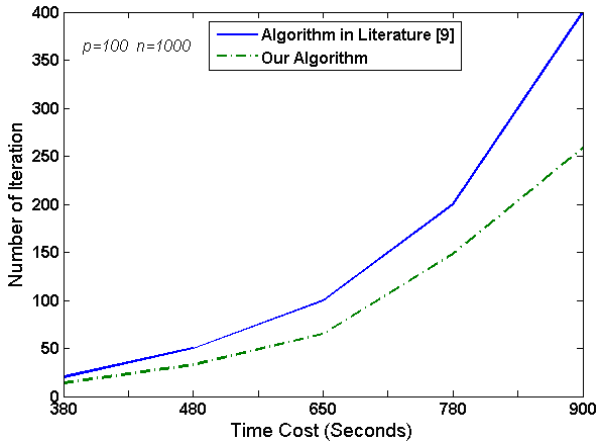

Fig. 5. Comparison of our method and algorithm in [10]

V. CONCLUSION

In this paper, we presented a technique for image fusion based on NSCT and ANMF model. The accelerated NMF method modifies the previous update rules of *W* and *H*, which achieves better effect by adopting the theory of matrix decomposition. The current approaches on the basis of NMF usually need more iterations to converge than proposed method, but the contented result can be attained by our technique via less iterations. The results of simulation experiments show that the proposed algorithm can not only reduce computational complexities, but achieve better performances than other mentioned techniques both in visual point and statistics.

ACKNOWLEDGMENT

This paper is sponsored by the Foundation of Jiangxi Educational Committee (GJJ10478).

REFERENCES

[1] Do M. N., Vetterli M. "The Contourlet Transform: an Efficient Directional Multi-resolution Image Representation". IEEE Transactions on Image Process. 14(12):2091–2106, 2005.

[2] Cunha A. L., Zhou J. P., Do M. N. "The Non-subsampled Contourlet Transform: Theory, Design and Applications". IEEE Transactions on Image Process. 15(10):3089–3101,2006.

[3] Qu X. B., Yan J. W., Yang G. D. "Multi-focus Image Fusion Method of Sharp Frequency Localized Contourlet Transform Domain based on Sum-modified-laplacian". Opt. Precision Eng.17(5):1203–1211,2009.

[4] Lee D. D., Seung H. S. "Learning the Parts of Objects by Nonnegative Matrix Factorization" Nature. 401(6755):788–791,1999.

[5] Miao Q. G., Wang B. S. "Multi-focus Image Fusion based on Nonnegative Matrix Factorization" Acta Optica Sinica. 25(6):755–759,2005.

[6] Novak M., Mammone R. "Use of Non-negative Matrix Factorization for Language Model Adaptation in a Lecture Transcription Task". Proc. of IEEE International Conference on Acoustics, Speech and Signal Processing. - Salt Lake, P. 541-544,2001.

[7] Guillamet D., Bressan M., Vitria J. "A Weighted Non-negative Matrix Factorization for Local Representations". Proc. of IEEE Computer Society Conference on Computer Vision and Pattern Recognition. - Kauai, 942-947,2001.

[8] Feng T., Li S. Z., Shun H. Y. "Local Non-negative Matrix Factorization as a Visual Representation". Proc. of 2nd International Conference on Development and Learning. - Cambridge, P.1-6, 2002.

[9] Michael M., Zhang Y. "An Interior-point Gradient Method for Large-scale Totally Nonnegative Least Squares Problems".International Journal of Optimization Theory and Applications. 126(1):191–202, 2005.

[10] Li L., Zhang Y. J. "A Survey on Algorithms of Non-negative Matrix Factorization".Acta Electronica Sinica. 36(4):737–742, 2008.

[11] Anjali M., Bhirud S. G. "Objective Criterion for Performance Evaluation of Image Fusion Techniques"International Journal of Computer Applications. 11(5):57–60, 2010.

[12] Rockinger O. "Pixel-level fusion of image sequences using wavelet frames". Proceedings of Image Fusion and Shape Variability Techniques. P.149–154, 1996.

[13] Gonzalez A M, Saleta J L, Catalan R G, Garcia R. "Fusion of multispectral and panchromatic images using improved IHS and PCA mergers based on wavelet decomposition". IEEE Transactions on Geoscience and Remote Sensing, 42(6):1291–1299,2004,